Article

Role of Sulfide Radical Cations in Electron Transfer Promoted Molecular Oxygenations at Sulfur

Edward L. Clennan, and Chen Liao

J. Am. Chem. Soc., **2008**, 130 (12), 4057-4068 • DOI: 10.1021/ja710301s

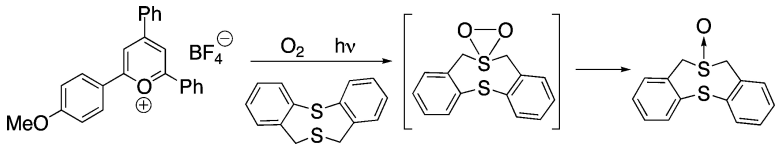

More About This Article

Additional resources and features associated with this article are available within the HTML version:

- Supporting Information
- Links to the 1 articles that cite this article, as of the time of this article download
- Access to high resolution figures
- Links to articles and content related to this article
- Copyright permission to reproduce figures and/or text from this article

View the Full Text HTML

J|A|C|S
ARTICLES
Published on Web 02/29/2008

Role of Sulfide Radical Cations in Electron Transfer Promoted Molecular Oxygenations at Sulfur

Edward L. Clennan* and Chen Liao

Department of Chemistry, University of Wyoming, 1000 East University Avenue, Laramie, Wyoming 82071

Received November 20, 2007; E-mail: clennane@uwyo.edu

Abstract: The methylene blue, *N*-methylquinolinium tetrafluoroborate, and pyrylium-cation-sensitized photooxygenations of 5H, 7H-dibenzo[b,g] [1,5]dithiocin, **1**, and 1,5-dithiacyclooctane, **2**, have been investigated. The methylene blue sensitized reactions exhibit all of the characteristics of a singlet oxygen reaction including isotope effects for the formation of a hydroperoxysulfonium ylide and the ability of **1** and **2** to quench the time-resolved emission of singlet oxygen at 1270 nm. The product compositions in the *N*-methylquinolinium tetrafluoroborate and pyrylium-cation-sensitized reactions are dramatically *different* and are both different from that anticipated for the participation of singlet oxygen. This argues for different reaction mechanisms for all three sensitizers. However, both the quinolinium and pyrylium-cation-sensitized reactions display all of the characteristics of electron-transfer-initiated photooxygenations. Both sensitizers were quenched at nearly diffusion-limited rates by **1** and **2**. Laser flash photolysis of mixtures of either sensitizer and **1** or **2** resulted in direct observation of the reduced sensitizer and the sulfide radical cation. In addition, electron-transfer reactions involving both sensitizers were shown to be exergonic. These results are consistent with the previously proposed outer sphere electron-transfer mechanism for *N*-methylquinolinium tetrafluoroborate and were used to argue for a new inner sphere mechanism for the pyrylium cation reactions.

Dioxygen is one of the most economical and environmentally friendly reagents available for functionalization of organic molecules to produce value-added products. These value-added oxidized organic substrates are important feedstock for the chemical and pharmaceutical industries. Unfortunately, many organic substrates of interest are notoriously resistant to molecular oxygenations with ground state triplet oxygen ($^3\Sigma_g$) under environmentally benign and easily controlled conditions. This problem has been circumvented in many cases by either activating oxygen or activating the substrate. Activation of oxygen has been achieved by either energy transfer to form singlet oxygen ($^1\Delta_g$) or by electron transfer to form superoxide ($O_2^{\bullet}$). Activation of organic substrates has been achieved by either electron transfer to form radical cations or anions or by hydrogen transfer to form radicals.

The reactions of organic sulfides with singlet oxygen have been extensively studied since first reported by Schenck and Krauch in the early 1960s.[1] Experimental evidence that two intermediates were involved on the potential energy surfaces of these reactions, on the way to the sulfoxide major products, was subsequently provided by Foote and co-workers in the 1970s and early 1980s.[2−5] Computational studies by Jensen and co-workers[6−9] suggested that the first intermediate is a persulfoxide (PS, Scheme 1) and the second intermediate a hydroperoxysulfonium ylide (HPY, Scheme 1). The persulfoxide suggestion was supported by trapping studies with substituted sulfoxides that established it as a nucleophilic oxygen transfer agent.[3] The hydroperoxysulfonium ylide suggestion replaced a previous assumption that the second intermediate was a thiadioxirane (TD, Scheme 1). It was demonstrated computationally that the activation barrier separating the persulfoxide and hydroperoxysulfonium ylide was far more consistent with experimental results than the barrier between the persulfoxide and thiadioxirane.[9] The hydroperoxysulfonium ylide suggestion was supported experimentally by trapping experiments that established its electrophilic oxygen transfer character, by isotope effect studies employing α-deuterium substituted sulfides,[10,11] and in an examination of the reactions of *β*-chlorosulfides.[12]

In 1977, Foote and co-workers[13] suggested that sulfide radical cations[14] were involved in the 9,10-dicyanoanthracene (DCA) photooxygenations of diethyl- and diphenylsulfide (Scheme 2). It has occasionally been assumed that the intermediate, R_2SO_2,

(1) Schenck, G. O.; Krauch, C. H. *Angew. Chem.* **1962**, *74*, 510.
(2) Foote, C. S.; Peters, J. W. *J. Am. Chem. Soc.* **1971**, *93*, 3795−3796.
(3) Gu, C.; Foote, C. S.; Kacher, M. L. *J. Am. Chem. Soc.* **1981**, *103*, 5949−5951.
(4) Gu, C.-L.; Foote, C. S. *J. Am. Chem. Soc.* **1982**, *104*, 6060−6063.
(5) Liang, J.-J.; Gu, C.-L.; Kacher, M. L.; Foote, C. S. *J. Am. Chem. Soc.* **1983**, *105*, 4717−4721.
(6) Jensen, F. *J. Org. Chem.* **1992**, *57*, 6478−6487.
(7) Jensen, F. Theoretical Aspects of the Reactions of Organic Sulfur and Phosphorus Compounds with Singlet Oxygen. In *Advances in Oxygenated Processes*; Baumstark, A. L., Ed.; JAI Press: Greenwich, CT, 1995; Vol. 4, pp 1−48.
(8) Jensen, F.; Foote, C. S. *J. Am. Chem. Soc.* **1988**, *110*, 2368−2375.
(9) Jensen, F.; Greer, A.; Clennan, E. L. *J. Am. Chem. Soc.* **1998**, *120*, 4439−4449.
(10) Clennan, E. L.; Liao, C. *Tetrahedron* **2006**, 10724−10728.
(11) Toutchkine, A.; Clennan, E. L. *J. Org. Chem.* **1999**, *64*, 5620−5625.
(12) Toutchkine, A.; Clennan, E. L. *Tetrahedron Lett.* **1999**, *40*, 6519−6522.

Scheme 1

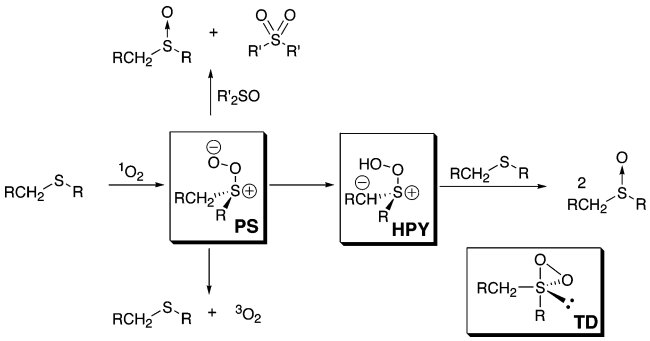

in this reaction is the persulfoxide, PS, and that its subsequent transformation to product occurs in an identical fashion to that observed in the singlet oxygen reaction (Scheme 1).[15,16] However, Baciocchi and co-workers[17] discovered in 2003 that diphenylsulfoxide does not trap any intermediate formed in the *N*-methylquinolinium tetrafluoroborate (NMQ^+)-sensitized photooxygenations of sulfides. This led to the suggestion that NMQ^+ sensitization, via the mechanism previously established for DCA (Scheme 2), does not proceed via a persulfoxide, PS, but that superoxide and the sulfide radical cation collapse directly to a thiadioxirane, TD.

Scheme 2

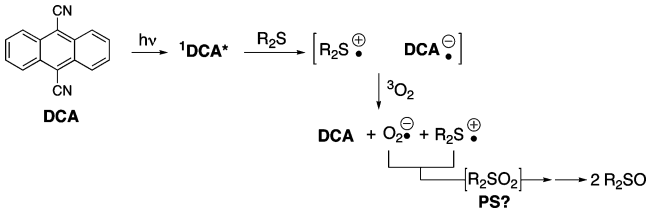

One-electron reduced DCA and NMQ^+ are both thermodynamically capable of reducing oxygen to superoxide as required by the mechanism in Scheme 2. On the other hand, it has been established that 2,4,6-triarylpyrylium tetrafluoroborates, TPP^+s, (Scheme 3), which form radicals incapable of producing superoxide, also catalyze sulfide photooxygenation reactions.[18,19] To rationalize these non-superoxide photooxygenations, Che[18] and Memarian[19] both suggested mechanisms initiated by direct reaction of the sulfide radical cation with oxygen to give a persulfoxide radical cation, PS• (Scheme 3). In the Che mechanism, formation of the persulfoxide, PS, is circumvented by direct formation of the thiadioxirane, TD, from pyrylium radical reduction of the persulfoxide radical cation, PS•, intermediate.

In 2006, Albini and co-workers pointed out that unproductive electron transfers between superoxide and sulfur radical cations are substantially more exothermic than reactions that form the thiadioxiranes, TD.[20] Consequently, they argued that superoxide is a byproduct not involved in product formation, and they suggested an alternative unitary chain-reaction mechanism for all of the sensitizers, as depicted in Scheme 4. This mechanism, as well as the mechanisms of Che and Memarian (Scheme 3), invoke direct reaction between a sulfide radical cation and oxygen, a reaction that has not been observed on the pulse radiolysis time scale.[21,22] In addition, a computational study of Rauk[23] does not characterize dimethylpersulfoxide radical cation, PS•, as a covalently bound species but rather as a loose ion-induced dipole complex bound by 3.2 kcal/mol with a sulfur−oxygen distance only slightly shorter than the sum of the van der Waals radii. Albini and co-workers[20] got around this latter problem by pointing out that addition of the ion−dipole complex to R_2S (step k_{R_2S} in Scheme 4) is highly exergonic and drives the entire reaction sequence.

Given the central role that oxidations of methionine residues in proteins play in a variety of degenerate diseases including Alzheimer's disease, we have undertaken a careful study of the photooxygenations of organic sulfides under a variety of conditions. We report here our results with 5H, 7H-dibenzo-[b,g] [1,5]dithiocin, **1**, and 1,5-dithiacyclooctane, **2**, with different sensitizers. These sensitizers react to provide unique product compositions and leave very different footprints with an arsenal of mechanistic tools. This pattern recognition approach provides compelling evidence for different sensitizer-dependent reactions and rules out the concept of a single unitary electron-transfer photooxygenation mechanism.

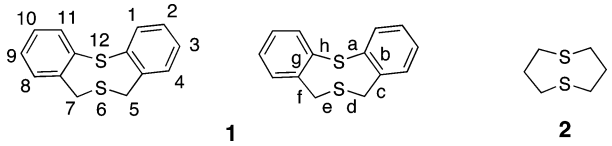

Results

The synthesis of 5H, 7H-dibenzo[b,g] [1,5]dithiocin, **1**, is shown in Scheme 5.[24] The proton NMR spectrum of **1** exhibits a large AB quartet and a smaller singlet (relative intensity singlet/AB quartet = 0.11) consistent with the previous suggestion that it exists in two non-interconverting conformations on the NMR time scale.[24] DFT calculations (B3LYP/6-31G(d)) located both C_s symmetric boat−chair (BC) and C_2 symmetric twist−boat (TB) conformational minima (Figure 1). The BC conformation is 2.23 kcal/mol more stable than the TB conformation. The small singlet broadened as the temperature of the NMR sample was lowered and then sharpened to form an AB quartet consistent with slow interconversion between the TB mirror images at low temperature. A complete line shape fit gave $\Delta G^{\neq}$ (228.16 K) = 10.4 kcal/mol, $\Delta H^{\neq}$ = 7.1 kcal/mol, and $\Delta S^{\neq}$ = −14.4 cal/mol·K, in reasonable agreement with $\Delta G^{\neq}$ (228.16 K) = 10.9 kcal/mol that was determined for this dynamic process by

(13) Eriksen, J.; Foote, C. S.; Parker, T. L. *J. Am. Chem. Soc.* **1977**, *99*, 6455−6456.
(14) Glass, R. S. Sulfur Radical Cations. In *Organosulfur Chemistry II*; Page, P. C. B., Ed.; Springer-Verlag: Berlin, 1999; Vol. 205, pp 1−87.
(15) Baciocchi, E.; Crescenzi, C.; Lanzalunga, O. *Tetrahedron* **1997**, *53*, 4469−4478.
(16) Akasaka, T.; Ando, W. *Tetrahedron Lett.* **1985**, *26*, 5049−5052.
(17) Baciocchi, E.; Del Giacco, T.; Elisei, F.; Gerini, M. F.; Guerra, M.; Lapi, A.; Liberali, P. *J. Am. Chem. Soc.* **2003**, *125*, 16444−16454.
(18) Che, Y.; Ma, W.; Ji, H.; Zhao, J.; Zang, L. *J. Phys. Chem. B* **2006**, *110*, 2942−2948.
(19) Memarian, H. R.; Mohammadpoor-Baltork, I. Bahrami, K. *Bull. Korean Chem. Soc.* **2006**, *27*, 106−110.
(20) Bonesi, S. M.; Manet, I.; Freccero, M.; Fagnoni, M.; Albini, A. *Chem.−Eur. J.* **2006**, *12*, 4844−4857.
(21) Schäfer, K.; Bonifacic, M.; Bahnemann, D.; Asmus, K.-D. *J. Phys. Chem.* **1978**, *82*, 2777−2780.
(22) Schöneich, C.; Aced, A.; Asmus, K.-D. *J. Am. Chem. Soc.* **1993**, *115*, 11376−11383.
(23) Huang, M. L.; Rauk, A. *J. Phys. Chem. A* **2004**, *108*, 6222−6230.
(24) Gellatly, R. P.; Ollis, W. D.; Sutherland, I. O. *J. Chem. Soc., Perkin Trans. II* **1976**, 913−925.

Scheme 3

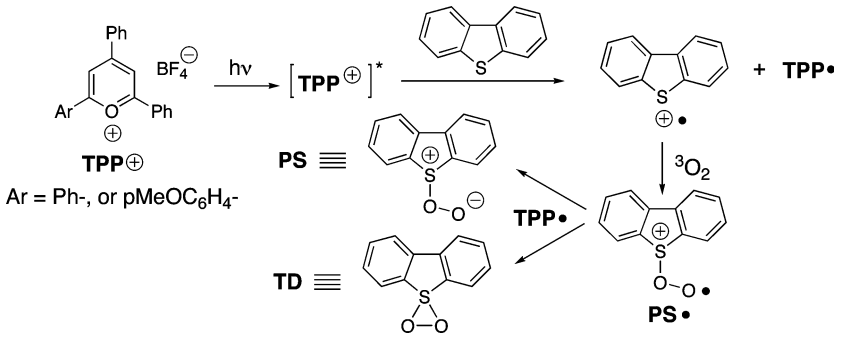

Scheme 4

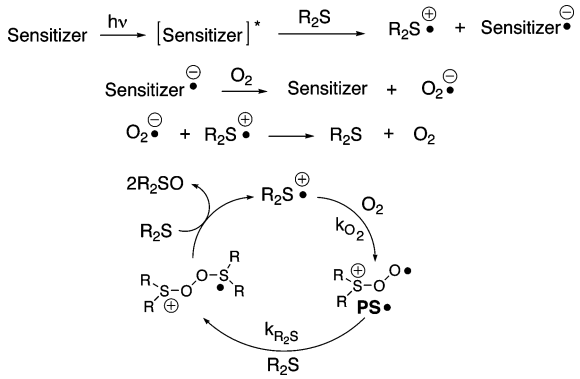

fitting a broadened spectrum at a single temperature.[24] The singlet and AB quartet observed at room temperature also began to broaden as the temperature was raised consistently with the onset of interconversion between the BC and TB conformations on the NMR time scale. All of these dynamic events were reversible, consistent with their conformational origin.

Methylene Blue Photosensitized Reaction of 1. An oxygen-saturated CD_3CN solution 1.1×10^{-2} M in **1** and 1×10^{-4} M in methylene blue containing 8.75×10^{-3} M benzyl benzoate as an internal standard was irradiated with a 600 W halogen−tungsten lamp through 1 cm of a saturated $NaNO_2$ filter solution. The major product of the reaction is 5H, 7H-dibenzo[b,g] [1,5]-dithiocin-6-oxide, **3**, with a small amount of 5H, 7H-dibenzo-[b,g] [1,5]dithiocin-6,6-dioxide, **4**, and a trace of *trans*-5H, 7H-

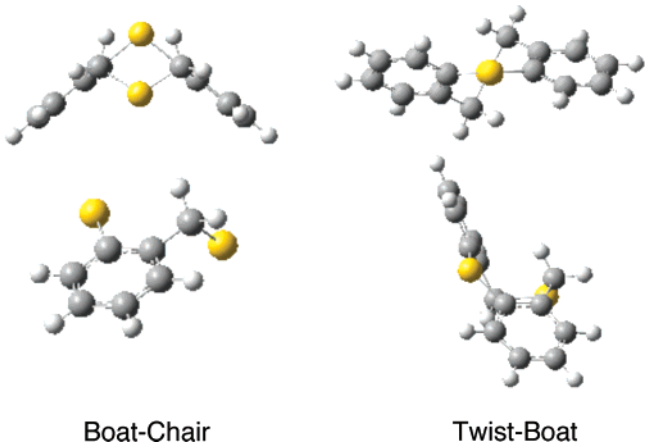

Figure 1. Boat−chair (BC) and C_2 symmetric twist−boat (TB) conformational minima of 5H, 7H-dibenzo[b,g] [1,5]dithiocin, **1**.

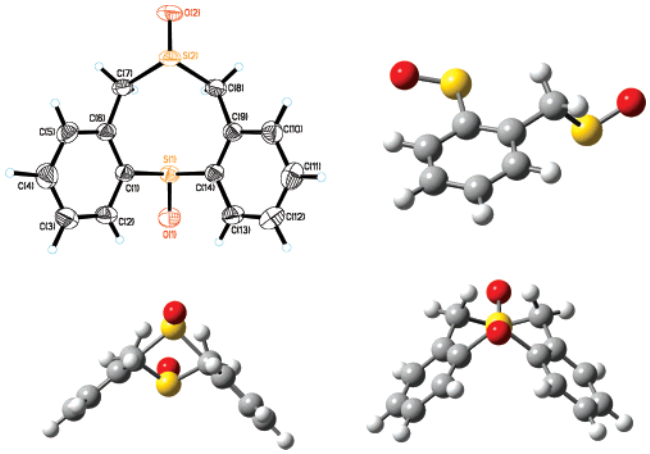

Figure 2. ORTEP plot and three ball-and-stick projections of the X-ray structure of bissulfoxide, **5**.

Scheme 5

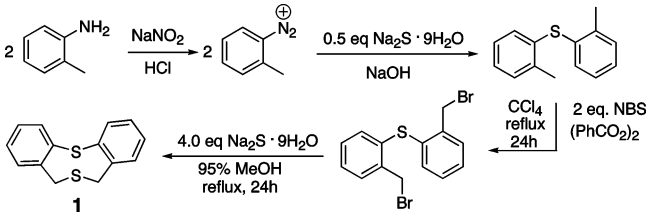

dibenzo[b,g] [1,5]dithiocin-6,12-dioxide, **5**, appearing after extended irradiation (eq 1). The *trans*-configuration of dioxide, **5**, was established by X-ray diffraction of an independently synthesized sample that was shown to be identical to the material formed in the photooxygenation (Figure 2). The dioxide adopts a BC conformation in the crystal with two equatorial-like oxygens. This isomer is the most stable of a set of four BC and three TB 6,12-dioxides that were located by density functional calculations (DFT) using the B3LYP/6-31G(d) model (Supporting Information).

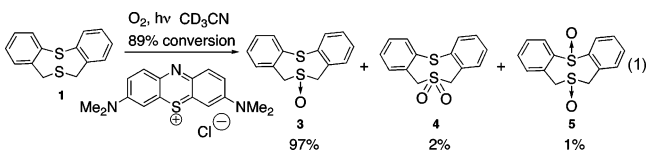

The proton NMR spectrum of sulfoxide **3** was more complex than previously reported.[25] Rather than two AB quartets, a set of three AB quartets between 3.8 and 5.6 ppm were observed in a 1.0:0.26:0.14 ratio at 400 MHz. This suggests that at

(25) Ohkata, K.; Okada, K.; Akiba, K. *Heteroat. Chem.* **1995**, *6*, 145−153.

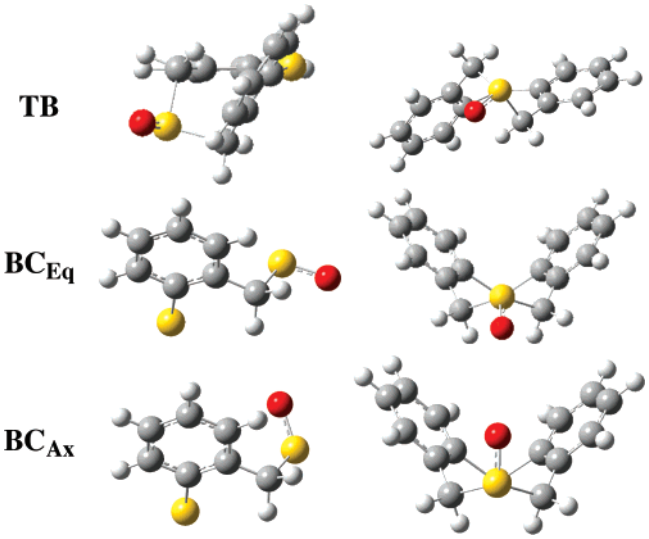

Figure 3. Two views of the twist−boat, TB, and boat−chair, BC, conformations of **3**.

least three conformational isomers of **3** are significantly populated. This suggestion was verified by B3LYP/6-31G(d) calculations that located two BCs, one with an axial-like sulfoxide oxygen, BC_{Ax}, and a second with an equatorial-like oxygen, BC_{Eq}, and a TB conformation. (Figure 3) A comparison of the zero point corrected energies reveal a stability sequence BC_{Eq} > TB > BC_{Ax}. Conversion of these energies, after adjusting the energy of the chiral TB conformation for the entropy of mixing, gives a population ratio TB/BC_{Eq}/BC_{Ax} of 1.0:0.55:0.06. The remarkable similarity of this calculated population ratio to the experimental ratio, 1.0:0.26:0.14, provides compelling confirmation of the assignment of the three AB quartets to three conformational isomers. In addition, all three AB quartets collapsed to a broad singlet when a DMSO-d_6 sample of **3** was heated to 120 °C in the probe of a 400 MHz NMR. These spectral changes were completely reversible, consistent with a dynamic interconversion of three conformational isomers.

Singlet oxygen was identified as the key oxidant in this reaction (eq 1) by DABCO quenching experiments that completely suppressed product formation and by trapping

Scheme 6

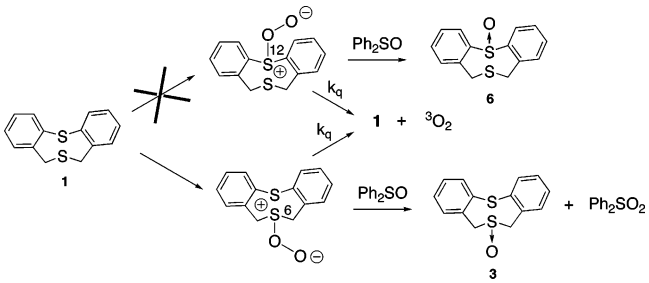

experiments with Ph_2SO that generated Ph_2SO_2 consistent with oxygen transfer from a persulfoxide intermediate. In the latter trapping experiments 5H, 7H-dibenzo[b,g][1,5]dithiocin-12-oxide, **6**, was not formed, suggesting that the 12-persulfoxide is not a transient intermediate that decomposes via physical quenching, k_q (Scheme 6). This is consistent with the known lack of reactivity of diphenylsulfide with singlet oxygen.

The formation of the well-established persulfoxide singlet oxygen adduct during the reaction of 1,5-dithiacyclooctane, **2**, was independently demonstrated by the photooxygenation of 2,2,8,8-tetradeuterio-1,5-dithiacyclooctane, **2**d_4.[10] In this case the product isotope effect ([**2**SOh_4]/[**2**SOd_4]) of 1.23 ± 0.08 reflects preferential formation of OOH in comparison to OOD (Scheme 7) as a result of the increased difficulty of abstraction of deuterium and concomitant more favorable partitioning along the physical quenching pathway, k_q, of persulfoxide PSHγ in comparison to persulfoxide PSHα.

The total rate constants, k_T, for reactions of **1** and **2** with singlet oxygen were extracted from the observed pseudo first-order rate constants for quenching of singlet oxygen phosphorescence at 1270 nm (Figure 4) by plotting k_{obs} versus the concentrations of the sulfide (Inset Figure 4; $k_{obs} = k_T$[sulfide] + k_d). The derived k_T, which represents the rate constant of all chemical, k_r, and physical, k_q, sulfide-induced pathways for the deactivation of singlet oxygen, was more than 30 times smaller for **1** ($k_T = [6.7 \pm 0.4] \times 10^5 M^{-1}s^{-1}$) than for **2** ($k_T = [2.1 \pm 0.2] \times 10^7 M^{-1}s^{-1}$). The reduced rate of the reaction of **1** in comparison to **2** is anticipated based upon the shielding of the bottom face of the molecule by the phenyl rings in the most stable butterfly-like BC conformation (Figure 1) and the known lack of reactivity of Ph_2S with singlet oxygen.

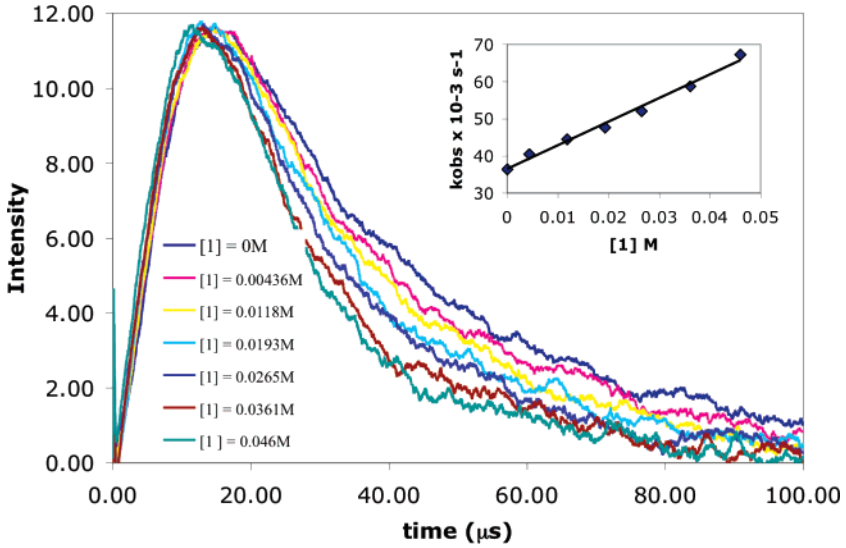

Figure 4. Time-resolved emission of singlet oxygen at 1270 nm as a function of the concentration of **1**. Inset, plot of the pseudo-first-order rate constants derived by fitting the decay curves versus the concentration of **1**.

Scheme 7. Reaction of **2**d_4 with Singlet Oxygen

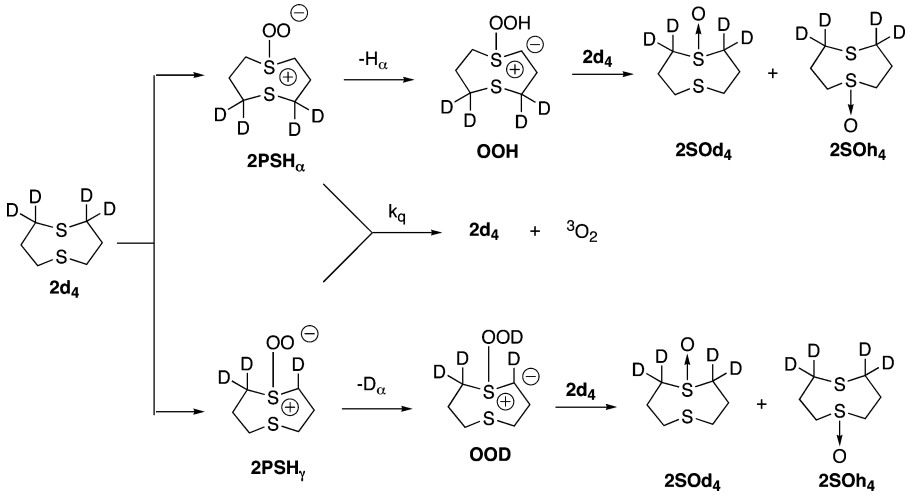

***N*-Methylquinolinium Tetrafluoroborate ($NMQ^+BF_4^-$) Photosensitized Reaction of 1.** Steady-state photolysis of a CD_3CN solution of **1** in the presence of 5 mol % $NMQ^+BF_4^-$ was conducted under constant agitation with oxygen by irradiation with a 450 W medium-pressure mercury lamp through a pyrex filter. NMR analysis revealed the formation of both **3** and **5**, which previously were observed in the methylene blue reaction, and a new product that was identified as 5H, 7H-dibenzo[b,g][1,5]dithiocin-12-oxide, **6**, by comparison to an authentic sample (eq 2). Product formation was quenched by *para*-benzoquinone, the well-established superoxide trap,[26] but not by DABCO. The absence of quenching by DABCO is especially significant because Baciocchi and co-workers[17] have previously demonstrated that $NMQ^+BF_4^-$ generates singlet oxygen. The absence of a singlet-oxygen component to this reaction is perhaps not surprising given the small rate constant (vide supra) for the singlet oxygen reaction.

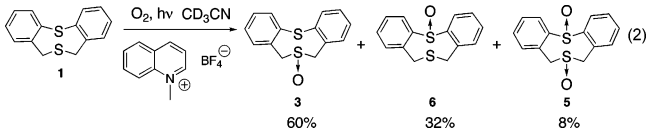

These results suggest the possibility that the NMQ^+ sensitized reaction of **1** occurs by an electron-transfer mechanism. The oxidation potential of **1** ($E°(D^+/D)$, eq 3) has not been reported, and a cyclic voltammetry study of **1** in CH_3CN with a platinum working electrode exhibited chemically irreversible behavior precluding determination of a thermodynamically significant oxidation potential. Nevertheless, using oxidation potentials of thianthrene (1.23 V vs SCE)[14,27] and 1,5-dithiacyclooctane (0.72 V vs SCE)[28,29] as limiting values in conjunction with the Rehm Weller equation[30] (eq 3), an estimate of a very exergonic free energy of electron transfer for **1** to the excited-state of $NMQ^+BF_4^-$ of $\Delta G_{et} = -33$ to -45 kcal/mol was obtained.[31]

$$\Delta G_{et}(\text{kcal/mol}^{-1}) = 23.06\{[E°(D^+/D) - E°(A/A^-)] - W_p - \Delta E_{00}\} \quad (3)$$

The ability of **1** to quench the fluorescence emission of NMQ^+ BF_4^- at 390 nm in acetonitrile is also consistent with an electron-transfer mechanism. The magnitude of the quenching rate constant of $2.23 \times 10^{10}M^{-1}s^{-1}$, which was derived from a Stern−Volmer analysis using a published value of 20 ns for the lifetime of singlet excited NMQ^+ BF_4^-,[32] is also similar to other electron-transfer rate constants measured for this sensitizer.[17] Finally, a laser flash photolysis study generated a transient absorption spectrum with two bands at 550 and 360 nm (Figure S17 in the Supporting Information). The 550 nm peak can be confidently assigned to $NMQ^•$ based upon comparison to the published spectrum of this radical and the sensitivity of this peak to quenching by oxygen. However, the transient at 360 nm, in contrast to $NMQ^•$, was not quenched by oxygen on the laser flash photolysis time scale, suggesting assignment of this higher energy band to $\mathbf{1}^{+•}$. Pyrylium salts absorb strongly at 360 nm, and their bleaching in laser flash photolysis studies obscure the absorbance of $\mathbf{1}^{+•}$ and preclude its direct observation in these experiments.

To provide independent confirmation of the assignment of the 360 nm peak to $\mathbf{1}^{+•}$, we have used the B3LYP/6-31G(d) model to locate stable conformations of $\mathbf{1}^{+•}$ and have calculated their absorption spectra using the time-dependent DFT method. Frequency calculations were used to verify the location of energy minima and the absence of spin contamination was checked by examination of $\langle S^2 \rangle$, which showed values acceptably close to 0.75 for these doublet cation radical species.[33] Three conformational minima were located and are depicted in Figure 5. The most stable conformation of $\mathbf{1}^{+•}$ is a twist−boat−boat conformation with C_1 symmetry that is characterized by a short sulfur−sulfur distance of 2.76 Å, well within the sum of two sulfur van der Waals radii of 3.6 Å.[34] The C_2 TB conformation is 2.91 kcal/mol above the global minimum and is characterized by a significant distance of 4.2 Å between the two sulfurs. The

(26) Manring, L. E.; Kramer, M. K.; Foote, C. S. *Tetrahedron Lett.* **1984**, *25*, 2523−2526.
(27) Zhao, B. J.; Evans, D. H.; Macias-Ruvalcaba, N. A.; Shine, H. J. *J. Org. Chem.* **2006**, *71*, 3737−3742.
(28) Wilson, G. S.; Swanson, D. D.; Klug, J. T.; Glass, R. S.; Ryan, M. D.; Musker, W. K. *J. Am. Chem. Soc.* **1979**, *101*, 1040−1042.
(29) Goto, Y.; Matsui, T.; Ozaki, S.; Watanabe, Y.; Fukuzumi, S. *J. Am. Chem. Soc.* **1999**, *121*, 9497−9502.
(30) Rehm, D.; Weller, A. *Isr. J. Chem.* **1970**, *8*, 259−271.
(31) The other values in eq 3 necessary to do this calculation are the reduction potential of the NMQ^+ ($E°(A/A^-) = -0.85$ V vs SCE), the singlet excited state energy of NMQ^+ ($\Delta E_{00} = 81.5$ kcal/mol), and the energy necessary to separate the ions, W_p, which is taken as zero in this case as a result of the lack of Coulombic interaction between the $NMQ^•$ radical and the sulfide radical cation.[49]
(32) Fukuzumi, S.; Fujita, M.; Noura, S.; Ohkubo, K.; Suenobu, T.; Araki, Y.; Ito, O. *J. Phys. Chem. A* **2001**, *105*, 1857−1868.
(33) Cramer, C. J. *Essentials of Computational Chemistry. Theories and Models*; John Wiley & Sons Ltd.: Chichester, England, 2002.
(34) Bondi, A. *J. Phys. Chem.* **1964**, *68*, 441−451.

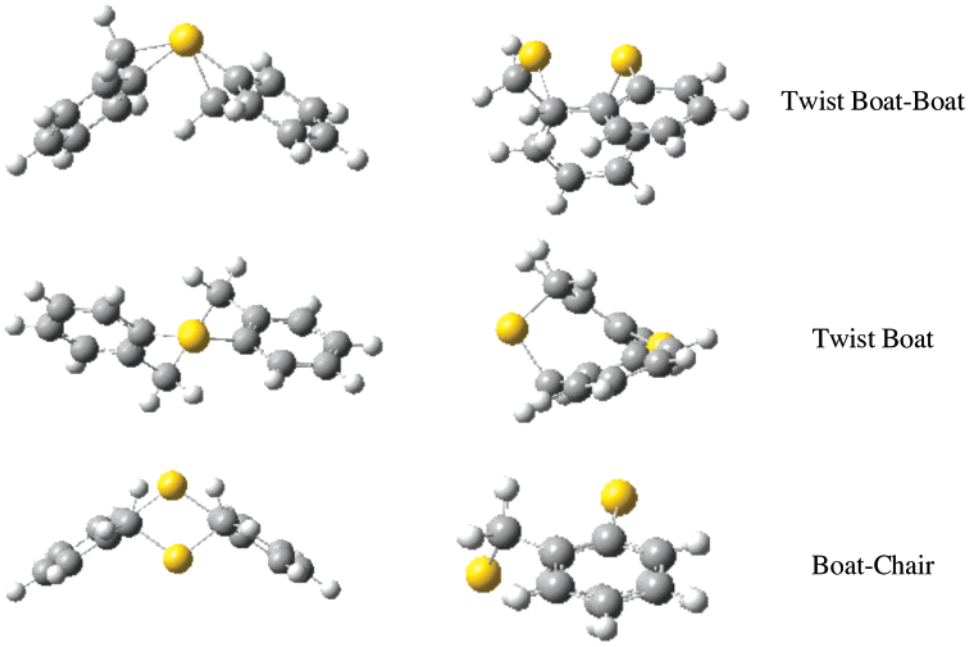

Figure 5. Two views of the B3LYP/6-31G(d) conformations of the radical cation of **1**.

C_S BC conformation is 9.16 kcal/mol above the global minimum and like the TB has a sulfur−sulfur distance (3.76 Å) greater than the sum of their van der Waals radii.

The time-dependent density functional theory (TD−DFT) calculations of the electronic spectra[35] of each of the radical cations were conducted both in the absence and presence of acetonitrile, using the polarization continuum model. The results are depicted in Figure 6 for the most stable twist−boat−boat conformation (Supporting Information for results on other conformations). The peak with the largest oscillator strength (*f*) in both the presence (378 nm, $f = 0.118$) and absence (375 nm, $f = 0.0774$) of acetonitrile is very close to the peak observed in the laser flash photolysis studies at 360 nm (vide supra). The long wavelength bands with low oscillator strength were not observed because of their low intensities and their wavelengths that were outside of our observation window.

To establish the reliability of this time-dependent DFT B3LYP/6-31G(d) model to calculate the absorption maximum we have also computationally examined 1,5-dithiacyclooctane radical cation, $\mathbf{2}^{+\bullet}$, because it has been directly observed and has an absorption maximum at 405 nm in acetonitrile.[36] This study led to the location of the BC, chair−chair, and boat−boat conformations that had been previously identified[37] and a fourth much higher energy TB conformation (Figure 7). TD−DFT calculations on the BC global minimum faithfully reproduced the experimentally observed absorption peak (404 nm, $f = 0.1089$; 414 nm (CH_3CN), $f = 0.1543$), providing compelling verification of the veracity of this method for the study of 5H, 7H-dibenzo[b,g][1,5]dithiocin radical cation, $\mathbf{1}^{+\bullet}$.

Pyrylium Salt Photosensitized Reactions of 1. Steady-state photolysis of 12.5 mM solutions of **1** in the presence of 1 mM triarylpyrylium tetrafluoroborates, TPP, **2**MeO−TPP, or **2**MeO−

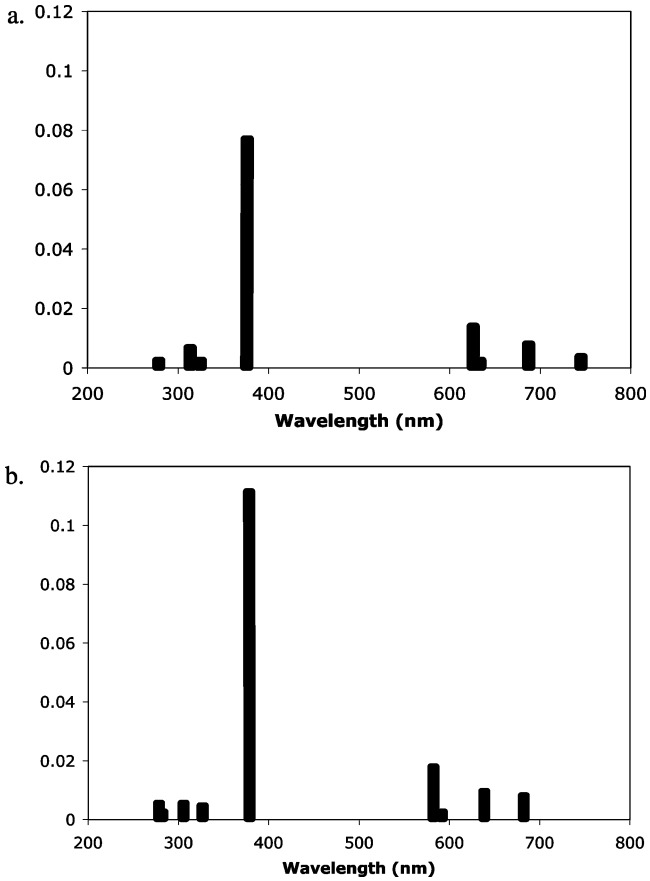

Figure 6. TD−DFT calculations on the B3LYP/6-31G(d)-minimized twist−boat−boat conformation of $\mathbf{1}^{+\bullet}$ in the (a) gas phase and (b) in CH_3CN.

STPP and 10 mM of benzylbenzoate as an internal standard in oxygen-saturated $CHCl_3$ led predominately to the formation of sulfoxide **3** (eq 4a). After extended irradiation, a trace (<1%) of an unknown product is produced, which we suspect is a ring cleavage product; however, its quantity precluded isolation and conclusive identification. Reaction of 1,5-dithiacyclooctane, **2**,

(35) Petersilka, M.; Grossmann, U. J.; Gross, E. K. U. *Phys. Rev. Lett.* **1996**, *76*, 1212−1215.
(36) Tamaoki, M.; Serita, M.; Shiratori, Y.; Itoh, K. *J. Phys. Chem.* **1989**, *93*, 6052−6058.
(37) Stowasser, R.; Glass, R. S.; Hoffmann, R. *J. Chem. Soc., Perkin Trans. 2* **1999**, 1559−1561.

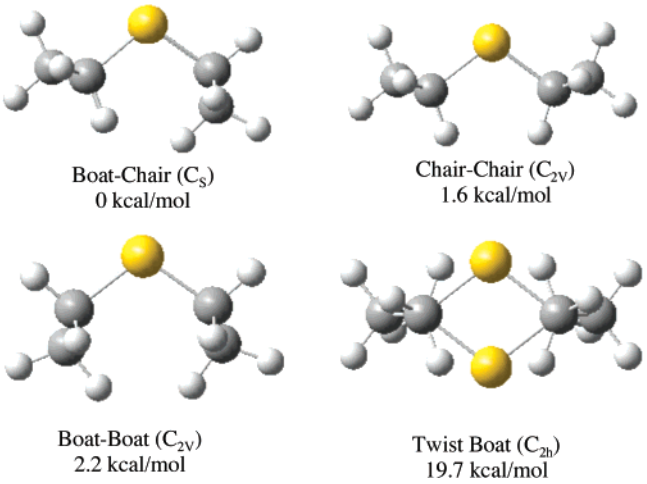

Figure 7. B3LYP/6-31G(d) energies and conformations of 1,5-dithiacyclooctane radical cation.

Table 1. Extent of Product Formation during Photooxygenation of **1** with Several Pyrylium Salts in CD_3CN and $CDCl_3$[a]

sensitizer	solvent	% product formation
TPP	$CDCl_3$	36.5
	CD_3CN	0
2MeOTPP	$CDCl_3$	28.9
	CD_3CN	14.0
2MeOSTPP	$CDCl_3$	58.6
	CD_3CN	6.8
STPP	$CDCl_3$	39.5
	CD_3CN	5.3

[a] Measured on a merry-go-round at a fixed irradiation time to allow comparison of percent conversions (percent product formation).

in CH_3CN produced a more complicated reaction mixture consisting of 1,5-dithiacyclooctane sulfoxide, **2**SO, and 1,5-dithiacyclooctane bissulfoxide, **2**SOSO (eq 4b). However, examination of this reaction as a function of time clearly shows that the bissulfoxide is a secondary product formed by over-oxidation of **2**SO.

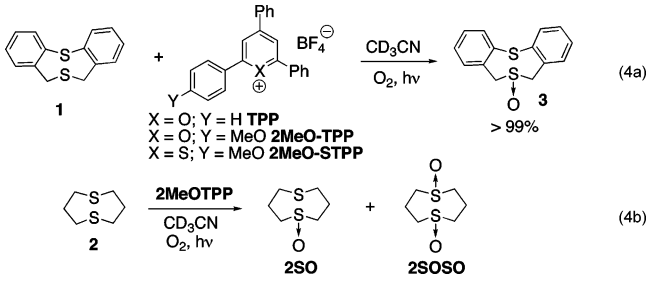

The photooxygenations of **1** with all of the pyrylium salt sensitizers were more rapid in the less polar $CDCl_3$ ($E_T(30)$ = 39.1 kcal/mol) than in the more polar CD_3CN ($E_T(30)$ = 46.0 kcal/mol)[38] (Table 1). Similar unusual solvent dependencies have previously been observed with electron-transfer reactions that generate radical/radical cation pairs that lack a Coulombic barrier to separation.[39] It has been suggested that back electron transfers, which decrease the efficiencies of these charge-shift reactions, are suppressed in the lower polarity solvents with smaller solvent reorganization energies (λ). This suggestion requires the back electron transfer to be in the Marcus inverted region, which is often the case and has recently been experimentally verified for the charge-shift reactions between tetralkyltins and acridinium ions.[40]

Rehm Weller analyses (eq 3) of the electron-transfer reactions suggested by these solvent effects for TPP (E_S = 65 kcal/mol, E_T = 53 kcal/mol, E^0(reduction) = −0.30V vs SCE in CH_3CN) and **2**MeOTPP (E_S = 55 kcal/mol[18], E^0(reduction) = −0.36 vs SCE in CH_3CN) indicate that the reaction of **1** is substantially exergonic with the singlet excited states of both sensitizers (TPP $\Delta G°$ = −30 to −41 kcal/mol; **2**MeOTPP $\Delta G°$ = −20 to −31 kcal/mol) and with the triplet excited-state of TPP ($\Delta G°$ = −17 to −28 kcal/mol). In addition, Stern−Volmer quenching of TPP (τ_S = 4.2 ns)[41] and of **2**MeOTPP (τ_S = 4.8 ns)[18] by both **1** (k_q = (2.14 ± 0.13) × 10^{10} $M^{-1}s^{-1}$ and k_q = (1.10 ± 0.01) × 10^{10} $M^{-1}s^{-1}$, respectively) and by **2** (k_q = (2.39 ± 0.12) × $10^{10}M^{-1}s^{-1}$ and (1.28 ± 0.01) × $10^{10}M^{-1}s^{-1}$, respectively) are all diffusion-controlled processes.

Nanosecond laser flash photolysis (LFP) studies of both TPP and **2**MeOTPP in an argon atmosphere in the presence of **1** also support an electron-transfer mechanism (Figure 8). In the TPP experiment, a transient species appears at 550 nm that can be safely assigned to the pyrylium radical (TPP•) based on literature precedent[42] (part a in Figure 8) We also assign the transient observed in the laser flash photolysis experiment of a mixture of **1** and **2**MeOTPP to the corresponding pyrylium radical by comparison to an electrochemically generated sample (Supporting Information for details).

Irradiations of **2**MeOTPP$^+BF_4^-$ and **2**MeOSTPP$^+BF_4^-$ did not produce an emission signal at 1270 nm attributable to sensitized formation of singlet oxygen ($^1\Delta_g$). The absence of a singlet oxygen component to this reaction was also verified by the absence of an isotope effect (k_H/k_D = 0.99 ± 0.03) in the **2**MeOTPP$^+BF_4^-$ sensitized reaction of **2**d_4 (Scheme 7).

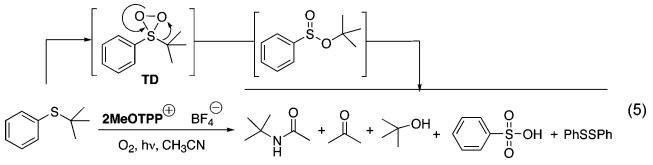

The **2**MeOTPP$^+BF_4^-$-sensitized photooxygenation of *tert*-butyl phenylsulfide (eq 5) generated a preponderance of cleavage products. Product formation was suppressed by 95 ± 5% in a nitrogen atmosphere in the presence of 1.2 × 10^{-3} M benzoquinone. In contrast, under identical reaction conditions only 50 ± 3% of the photooxygenation of **1** was quenched by 1.2 × 10^{-3}M benzoquinone. Baciocchi and co-workers[43] observed the same oxygen dependent cleavage of this sulfide using NMQ^+ and attributed it to rearrangement of a thiadioxirane intermediate.

(38) Reichardt, C. *Angew. Chem., Int. Ed. Engl.* **1979**, *18*, 98−110.
(39) Todd, W. P.; Dinnocenzo, J. P.; Farid, S.; Goodman, J. L.; Gould, I. R. *J. Am. Chem. Soc.* **1991**, *113*, 3601−3602.
(40) Fukuzumi, S.; Ohkubo, K.; Suenobu, T.; Kato, K.; Fujitsuka, M.; Ito, O. *J. Am. Chem. Soc.* **2001**, *123*, 8459−8467.
(41) Marin, M. L.; Miguel, A.; Santos-Juanes, L.; Arques, A.; Amat, A. M.; Miranda, M. A. *Photochem. Photobiol. Sci.* **2007**, *6*, 848−852.
(42) Akaba, R.; Niimura, Y.; Fukushima, T.; Kawai, Y.; Tajima, T.; Kuragami, T.; Negishi, A.; Kamata, M.; Sakuragi, H.; Tokumaru, K. *J. Am. Chem. Soc.* **1992**, *114*, 4460−4464.
(43) Baciocchi, E.; Del Giacco, T.; Giombolini, P.; Lanzalunga, O. *Tetrahedron* **2006**, *62*, 6566−6573.

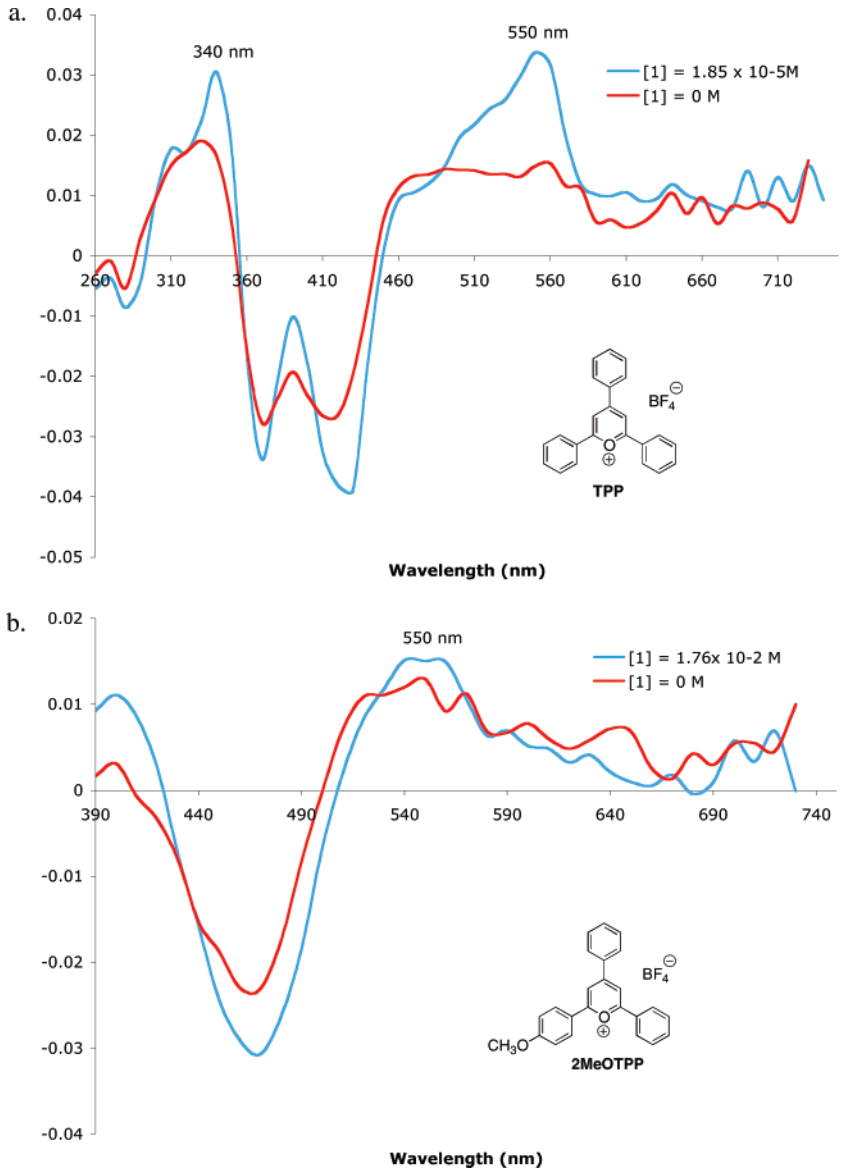

Figure 8. Laser flash photolysis of (a) TPP and (b) **2**MeOTPP at 355 nm in the absence and presence of **1**.

Discussion

The reactions of two 1,5-dithiacyclooctanes, **1** and **2**, have been examined with three different families of sensitizers, thiazines (Methylene Blue), quinolinium salts, and pyrylium cations.

Methylene Blue. Methylene Blue (MB) is a well-established singlet sensitizer[44,45] that promotes singlet oxygen reactions of sulfides by the mechanism shown in Scheme 1. However, the possibility of an electron-transfer pathway for the MB-sensitized reaction of easily oxidized **1** (eq 1) cannot be summarily discarded because Manring, Ericksen, and Foote[46] have provided convincing evidence for electron transfer in the MB photooxygenation of *trans*-stilbene. In this case, electron transfer occurs because of the well-recognized lack of reactivity of *trans*-stilbene toward singlet oxygen.[47,48] Nevertheless, an electron-transfer pathway for the MB-sensitized reactions of **1** and **2** can be ruled out and the well-established singlet oxygen pathway (Scheme 1) supported by several experimental observations. (1) Both **1** and **2** quench the 1270 nm emission of singlet oxygen with rate constants (**1**-[6.7 ± 0.4] × $10^5 M^{-1}s^{-1}$; **2**-[2.1 ± 0.2] × $10^7 M^{-1}s^{-1}$) much larger than that observed for *cis*-stilbene. (2) Product formation in the reactions of **1** and **2** are both quenched by the specific singlet oxygen quencher, DABCO. (3) The kinetic isotope effect observed in the MB-sensitized reaction of $\mathbf{2}d_4$ is consistent with intermediacy of a persulfoxide, a well-established intermediate in singlet-oxygen reactions of sulfides. (4) Oxidation is not observed (eq 1) at S_{12}, the sulfur directly attached to the two phenyl rings in **1**, consistent with the lack of reactivity of diphenylsulfide with singlet oxygen. (5) Diphenylsulfoxide, which is itself unreactive to singlet oxygen, is oxidized to diphenylsulfone in the presence of **1**,

(44) Stracke, F.; Heupel, M.; Thiel, E. *J. Photochem. Photobiol., A* **1999**, *126*, 51−58.
(45) Tanielian, C.; Golder, L.; Wolff, C. *J. Photochem.* **1984**, *25*, 117−125.
(46) Manring, L. E.; Eriksen, J.; Foote, C. S. *J. Am. Chem. Soc.* **1980**, *102*, 4275−4277.
(47) Eriksen, J.; Foote, C. S. *J. Am. Chem. Soc.* **1980**, *102*, 6083−6088.
(48) Wilkinson, F.; Helman, W. P.; Ross, A. B. *J. Phys. Chem. Ref. Data* **1995**, *24*, 663−1021. The rate constant for the reaction of *trans*-stilbene with singlet oxygen has not been reported; however, the rate constant for the reaction of *cis*-stilbene ($3 \times 10^3 M^{-1}s^{-1}$) is one of the smallest reported in the Wilkinson compilation of rate constants for over 1900 compounds.

Scheme 8

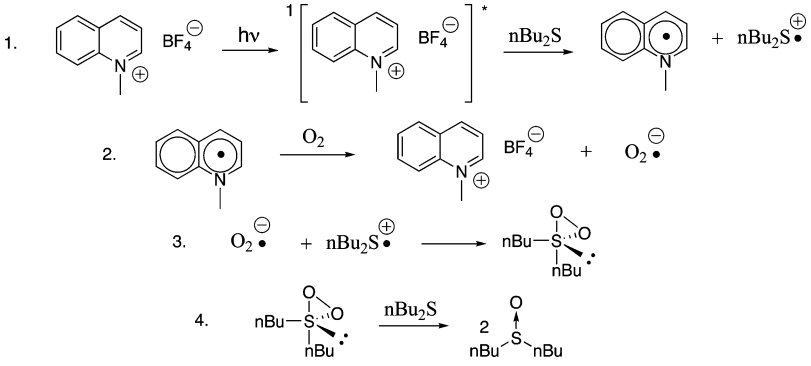

consistent with trapping a persulfoxide, a well-established intermediate, in the reactions of sulfides with singlet oxygen.

***N*-Methylquinolinium Tetrafluoroborate.** The *N*-methylquinolinium salt is a well-established potent electron-transfer sensitizer with a high singlet excited-state energy of 81.5 kcal/mol, a triplet excited-state energy of approximately 60.5 kcal/mol, and a reduction potential of −0.85 V versus SCE.[49] The triplet excited-state is not populated significantly by intersystem crossing from the singlet as revealed by a very high fluorescence quantum yield but is formed in the presence of oxygen in a process that produces singlet oxygen with a quantum yield of 2.0.[17] Baciocchi and co-workers,[17] however, provided convincing evidence that the $NMQ^+BF_4^-$-sensitized reaction of di-*n*-butylsulfide occurs by the electron-transfer mechanism depicted in Scheme 8. The key feature of this mechanism is the reaction between superoxide and the di-*n*-butylsulfide radical cation that generates the thiadioxirane (step 3 Scheme 8). This is also the step that distinguishes it from singlet-oxygen reactions that produce persulfoxide and hydroperoxysulfonium ylide intermediates (vide supra). The absence of a persulfoxide in this reaction was inferred from the inability to trap a nucleophilic intermediate with diphenylsulfoxide.

The experimental results obtained in the $NMQ^+BF_4^-$ sensitized reaction of **1** are also more consistent with a reaction via electron transfer than via singlet oxygen. For example, 5H, 7H-dibenzo[b,g][1,5]dithiocin-12-oxide, **6**, formed in the reaction of **1** with $NMQ^+BF_4^-$ (eq 2), is clearly not a singlet-oxygen product as established by the reaction with methylene blue (vide supra). This conclusion is confirmed by the inability of DABCO to quench the formation of **6**. The formations of **3** and **5** are also unaffected by the addition of DABCO to the $NMQ^+BF_4^-$/**1** reaction, suggesting that singlet oxygen is not involved in the formation of any of the reaction products. On the other hand, **1** quenches the fluorescence of $NMQ^+BF_4^-$ at a nearly diffusion controlled rate and laser flash photolysis unambiguously identifies the formation of NMQ•. These results coupled with a favorable calculated exergonicity suggest that reaction of **1** with $NMQ^+BF_4^-$ is initiated by electron transfer (Scheme 9). The rate constant for the chemical reaction of **1** with singlet oxygen, k_r, which must be no larger than the total rate constant ($k_T = k_r + k_q = [6.7 \pm 0.4] \times 10^5 M^{-1}s^{-1}$) for the removal of singlet oxygen from solution by **1** is clearly too small to compete with the electron-transfer pathway. Even di-*n*-butylsulfide, which reacts more rapidly with singlet oxygen ($k_T = 2.9 \times 10^7 M^{-1}s^{-1}$) than **1**, is preferentially oxidized by an electron-transfer mechanism in the presence of $NMQ^+BF_4^-$ (vide supra).

Scheme 9

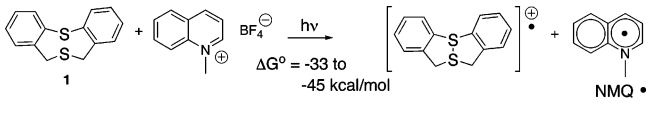

Triarylpyrylium Salts. The product distributions for the sensitized photooxygenations of **1** are very different for pyrylium salts and $NMQ^+BF_4^-$, which rule out the operation of any unitary mechanism for these sensitizers such as depicted in Scheme 4. In addition, the triarylpyrylium salts used in this study do not sensitize the formation of singlet oxygen. Consequently, we suggest the unique photooxygenation mechanism for these triarylpyrylium cations depicted in Scheme 10. The formation of the triplet excited-state of pyrylium cations (step 1, Scheme 10) is well established[50] and in many cases the triplet−triplet absorption can be observed by laser flash photolysis. The arguments for the charge-shift electron transfer (step 2, Scheme 10) are also compelling and include, (1) the fluorescence of TPP, and **2**MeO−TPP are quenched at diffusion-controlled rates by **1**, (2) electron transfers from **1** to the excited pyrylium salts

Scheme 10

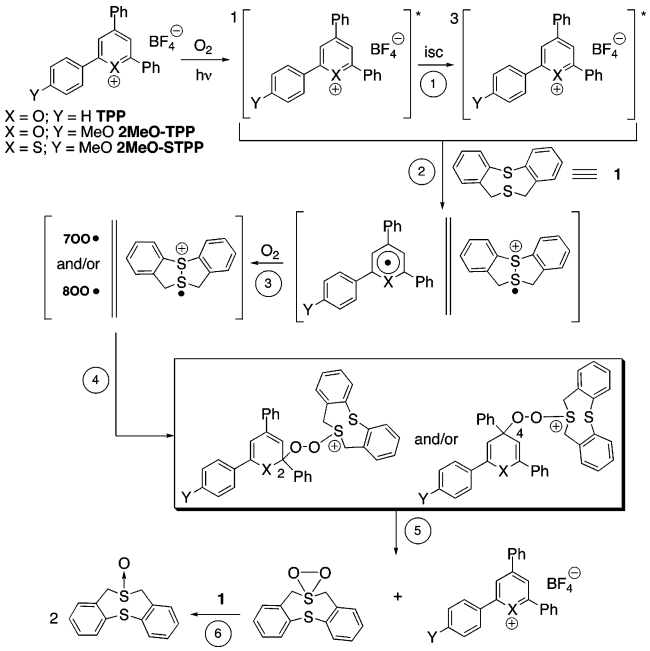

(49) Yoon, U. C.; Quillen, S. L.; Mariano, P. S.; Swanson, R.; Stavinoha, J. L.; Bay, E. *J. Am. Chem. Soc.* **1983**, *105*, 1204−1218.

(50) Miranda, M. A. *Chem. Rev.* **1994**, *94*, 1063−1069.

Scheme 11

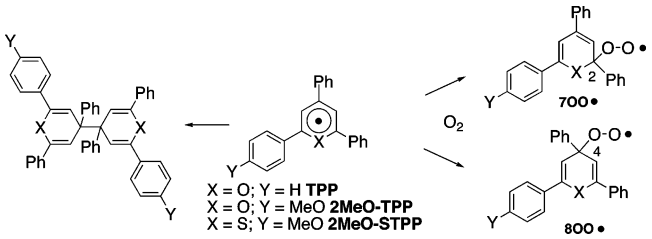

are exergonic, (3) the formation of the pyrylium radicals have been observed in laser flash photolysis experiments in the presence of **1**, and (4) the observed increases in reaction efficiencies with decreasing solvent polarity are diagnostic of charge-shift reactions.

Step 3 in Scheme 10 involves the addition of oxygen directly to the pyrylium radicals to form covalently bound peroxy radicals (Scheme 11). Pyrylium radicals TPP•, **2**MeOTPP•, and **2**MeOSTPP do not appear to react with oxygen on the LFP time scale; however, they do react on the cyclic voltammetry time scale (Figure S15 in the Supporting Information). It is the oxidations of these peroxy radicals that we suggest are responsible for the quenching of pyrylium-catalyzed photooxygenations by 1,4-benzoquinone. The trapping by benzoquinone leads directly to the pyrylium cation, oxygen, and the benzoquinone radical that subsequently reduces the sulfide radical cation. This oxidation competes with step 4, which is sterically slower for *tert*-butylphenyl sulfide than for **1**, which provides an explanation for the less effective quenching of the photooxygenation of **1**.

The reaction of **2**MeOTPP• with oxygen is a complicated process as revealed by the absence of an isosbestic point in the UV spectrum when electrochemically generated **2**MeOTPP• is exposed to oxygen (Figure S11 in the Supporting Information). The initially formed product is likely a peroxy radical formed by the addition of oxygen to either the 2 or 4 position of the radical (Scheme 11). It is well established that pyrylium radicals dimerize at the 4-position (Scheme 11);[52] however, B3LYP/6-31G(d) calculations (Supporting Information) identified three rotomeric minima for the 2-peroxy radical, **7**OO•, which are all 1 to 2 kcal/mol more stable than the 4-peroxy radical rotomers, **8**OO• (Figure S16 in the Supporting Information).

In step 4 (Scheme 10), these peroxy pyrylium radicals, **7**OO• and **8**OO•, add to the sulfide radical cation, located in close proximity within the same solvent cage, to form the alkylated persulfoxides shown in the box in Scheme 10. The other two possible alkylated persulfoxide isomers are not formed because the ortho hydrogens on the phenyl rings in the twist−boat−boat conformation of the radical cation of **1** effectively block the approach to S_{12}. Computational evidence for these alkylated persulfoxides was obtained by examining *O*-methyl dimethylpersulfoxide. Using this simple model, two alkylated persulfoxide rotomers, the bisected and anti conformations, have been located as energy minima at a variety of different computational levels (Table 2).

These unusual alkylated persulfoxides decompose to generate the thiadioxirane in step 5 (Scheme 10) concomitantly with

Table 2. Energy Differences between the Anti and Bisected Conformations of Methyl Dimethylpersulfoxide

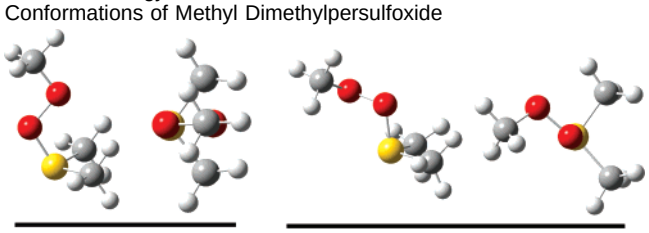

computational level	Δ*E* (anti-bisected), kcal/mol
MP2/6-31G(d)	1.94
MP2/6-311+G(d,p)	2.04
B3LYP/6-31G(d)	1.73
B3LYP/6-311+G(d,p)	1.89
B3LYP/6-311++G(3df,2dp)	1.83

restoration of the pyrylium cation resonance energy. Nucleophilic oxygen transfer to the sterically unencumbered S_6 sulfur in **1** subsequently generates two molecules of **3** as the exclusive product (step 6, Scheme 10). The oxygen-dependent pyrylium-sensitized cleavage of *tert*-butylphenyl sulfide (eq 5) provides the experimental evidence for the thiadioxirane as the key intermediate in this pyrylium catalyzed process. However, the thiadioxirane must be formed without the intermediacy of a persulfoxide intermediate because a product isotope effect ([**2**SOh$_4$]/[**2**SOd$_4$]) of 0.99 ± 0.03 was observed in the **2**MeOTPP$^+$-catalyzed photooxygenation of **2**d$_4$ (Scheme 7).

The direct formation of a thiadioxirane bypassing the formation of a persulfoxide intermediate suggests that the anti rotomer of the alkylated persulfoxide is the crucial reactive intermediate. The MP2/6-31G(d) bisected conformation of the alkylated persulfoxide has a core geometry nearly identical to the MP2/6-31G(d) geometry of the stable bisected persulfoxide (Figure 9) and would be expected to collapse to this product by a least-motion argument. On the other hand, the anti alkylated persulfoxide has a core geometry nearly identical to that of thiadioxirane (Figure 9) and very similar to the transition state for the formation of the thiadioxirane and is its likely precursor.[9] Indeed, removal of the methyl group from the MP2/6-31G(d) structure of anti-methyl dimethylpersulfoxide followed by geometry minimization leads directly to thiadioxirane. This is consistent with previous computational studies that failed to locate a stable anti persulfoxide.[9]

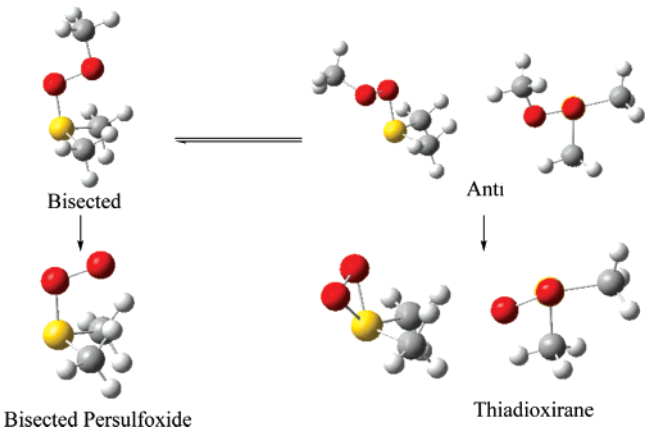

Figure 9. Reaction of the rapidly inteconverting bisected and anti alkylated persulfoxides to give the bisected persulfoxide and thiadioxirane, respectively.

(51) Sawyer, D. T. *Oxygen Chemistry*; Oxford University Press: New York, 1991; p 223.
(52) Wintgens, V.; Pouliquen, J.; Kossanyi, J.; Heintz, M. *Nouv. J. Chim.* **1986**, *10*, 345−350.

An alternative mechanism to that shown in Scheme 10 involves thermodynamically unfavorable formation of superoxide ($E°(O_2/O_2^{-\bullet})$ = −0.87 V vs SCE in CH_3CN)[51] by pyrylium radical (TPP$^\bullet$, **2**MeOTPP$^\bullet$, and **2**MeOSTPP$^\bullet$) reduction of oxygen that is driven by its rapid reaction with sulfide radical cation, or its formation by decomposition of **7**SOO$^\bullet$ and **8**SOO$^\bullet$, and its subsequent reaction via steps 3 and 4 in the Baciocchi mechanism[2] (Scheme 8). This would provide a rationale for the observed quenching by benzoquinone. However, the absence of the diagnostic superoxide product **6** formed in the NMQ^+-catalyzed reaction of **1** (eq 2) precludes this alternative possibility.

Conclusion

We have demonstrated that electron-transfer photooxygenations of sulfides are far more complex than previously assumed. Although the experimental data suggests that NMQ^+ functions as a simple outer sphere electron shuttle between the sulfide and oxygen, and pyrylium cations function by a less passive inner sphere mechanism. We also introduced a new technique, the photooxygenation of **2**d_4, to detect the absence of a persulfoxide in electron-transfer-catalyzed oxygenations and illustrated its use with the pyrylium cation sensitizer, **2**MeOTPP$^+$.

Experimental Section

Sulfides **1, 2**,[10] **2SO**,[10] **2SOd$_4$**,[10] **2d$_4$**,[10] **3**,[25] **4**,[25] **5**,[25] **6**,[25] and $NMQ^+BF_4^-$[53] were all synthesized as reported in the literature. Commercial samples of TPP, and **2**MeOTPP were used as received for the photochemical reactions and purified by recrystallization from ethanol for the electrochemical studies.

2-(*p*-Methoxyphenyl)-4,6-diphenyl-thiapyrylium Tetrafluoroborate. 2-MeO−STPP was synthesized using a modified procedure of Suld[54] and Wizinger.[55] A 2.5 mL H_2O solution of sodium sulfide nonahydrate (250 mg, 1.04 mmol) was added to a solution of **2**MeOTPP (0.21 g, 0.5 mmol) in 10 mL of acetone. After the addition was complete, the mixture was stirred for 0.5 h, then acidified with 2.5 mL of 48% HBF_4, diluted with 10 mL of H_2O, stirred for 2 h, and then filtered. The crude product was recrystallized twice from ethanol. Yield 11%. ^{1}H NMR (CD_3CN) δ 3.96 (s, 3H), 7.27(d, J = 8.7 Hz, 2H), 7.70−7.81(m, 6H), 8.07−8.17(m, 6H), 8.80(d, J = 14.7 Hz, 2H).

Radical Cation Preparation. Solutions of **1** and **2** were prepared in a specially designed two-compartment cell with one compartment filled with 0.1 M substrate and the second compartment with 1 equiv of sublimed (220 °C) $NOBF_4$ in acetonitrile. Both compartments were subjected to a series of three freeze−pump−thaw cycles and then mixed at room temperature under vacuum. The UV−vis spectra of **2**$^{+\bullet}$ was collected immediately. The yellow color of **1**$^{+\bullet}$ disappeared too rapidly to allow measurement of its UV−vis spectrum at room temperature.

Crystallographic Data for 5. X-ray diffraction data were collected for $C_{14}H_{12}S_2O_2$ on a Bruker P4 Diffractometer equipped with a molybdenum tube and a graphite monochromator at 25 °C. A colorless rectangular prismatic crystal of approximate dimensions 0.52 × 0.36 × 0.24 mm^3 glued to a glass fiber was used for data collection. A total of 2812 (R_{int} = 0.0226) independent reflections were gathered in the 2θ range of 4.04 to 55° with the data collected having $-1 \le h \le 9$, $-10 \le k \le 10$, $-13 \le l \le 13$ using the *XSCANS* program.[56] Three standard reflections measured after every 97 reflections exhibited no significant loss of intensity. The data were corrected for Lorentz-polarization effects and absorption. The structure was solved by Patterson methods and refined by least-squares techniques adapting the full-matrix weighted least-squares scheme, $w^{-1} = \sigma^2F_o^2 + (0.0596P)^2 + 0.17P$, where $P = (F_o^2 + 2F_c^2)/3$, on F^2 using the *SHELXTL* program.[57,58]

$C_{14}H_{12}S_2O_2$ crystallizes in the centrosymmetric triclinic space group $P\bar{1}$. The asymmetric unit consists of a compound molecule. The molecules are well ordered and well separated. All non-hydrogen atoms were located in the difference maps during successive cycles of least-squares and refined anisotropically. All of the hydrogen atoms except for one were located in the Fourier maps and refined isotropically. One of the hydrogen atoms was placed in a calculated position and refined isotropically using a riding model. The final refinement parameters were R_1 = 0.0364 and $wR2$ = 0.1015 for data with $F > 4\sigma(F)$, giving a data-to-parameter ratio of 12. The refinement data for all of the data were R_1 = 0.0403 and $wR2$ = 0.1050.

Laser Flash Photolysis. Nanosecond laser flash photolysis experiments were conducted using an excitation wavelength of 355 nm (5−20 mJ/pulse) from a Nd:YAG laser. The transient spectra were recorded with a point−point technique with 5−10 nm intervals from 350 to 700 nm. The kinetic decays were the average of at least 10 shots. Samples were degassed by either three freeze−pump−thaw cycles or by bubbling with argon. The optical densities were adjusted to between 0.3 and 0.6 at the excitation wavelength. When oxygen was needed, the sample was saturated with oxygen for 20 min. Several solvents were used including methylene chloride, 1,2-dichloroethane, and acetonitrile. In general, the most intense peaks were observed in 1,2-dichloroethane. The singlet-oxygen experiments were done with oxygen-saturated solutions using either the 355 or 532 nm output of a 10 Hz Nd:YAG laser. The kinetic apparatus consisted of a germanium (Judson 5 mm ϕ) diode detector/customized preamplifier and various optics: A 10 nm narrow band-pass non-fluoresceing filter centered at 1.27 μm placed just ahead of the detector, a 500 MHz LeCroy transient digitizer/signal averager interfaced to a computer, and an energy meter. Because the experimental decay is a convolution of the detector response (fwhm of approximately 10 ps for the 5 mm ϕ detector) and the sample decay, it was necessary to implement a numerical deconvolution analysis to accurately extract measured lifetimes 100 μs $\ge \tau \ge$ 2 ms from the recorded data. The numerical deconvolution analysis of Demas[59] for exponential decays corrects artifacts caused by scattered excitation light that may reach the detector that was used. This analysis was implemented on our laboratory computer using a general scientific/engineering analysis/data acquisition program called *Lifetime*. Signal averaging 100 experiments, each with laser pump energies ≤5 mJ gave 8192-point decay curves, each of which produced pseudo first-order rate constants with correlation coefficients (square root) better than 0.99.

Stern−Volmer Studies. All Stern−Volmer studies were done using acetonitrile as the solvent and sensitizer concentrations of [NMQ^+] = 1.5 × 10^{-5} M, [TPP^+] = 4 × 10^{-6} M, and [**2**MeOTPP$^+$] = 4 × 10^{-6} M. In the TPP^+ quenching studies, the concentrations of **1** were varied over the range of 5.16 × 10^{-4} to 9.82 × 10^{-3} M, the concentrations of **2** over the range of 5.7 × 10^{-4} to 5.7 × 10^{-3} M, and utilized an excitation wavelength of 405 nm and slit widths of 2.5 nm on the excitation side and 5 nm on the emission side. In the **2**MeOTPP$^+$ quenching studies, the concentrations of **1** were varied over the range of 2.0 × 10^{-3} to 8.7 × 10^{-3} M, the concentrations of **2** over the range of 6.6 × 10^{-4} to 7.9 × 10^{-3} M, and utilized an excitation wavelength of 447 nm and slit widths of 5.0 nm on both the excitation side and emission side. In the NMQ^+ quenching studies, the **1** concentrations were varied over the range of 2.5 × 10^{-4} to 1.5 × 10^{-3} M, and utilized an excitation wavelength of 317 nm and slit widths of 2.5 nm on the excitation side and 5 nm on the emission side. All slopes of the Stern−

(53) Donovan, P. F.; Conley, D. A. *J. Chem. Eng. Data* **1966**, *11*, 614−615.
(54) Suld, G.; Price, C. C. *J. Am. Chem. Soc.* **1962**, *84*, 2090−2094.
(55) Wizinger, R.; Ulrich, P *Helv. Chim. Acta* **1956**, *39*, 207−216.
(56) Bruker *XSCANS*, ver. 2.31; Bruker AXS: Madison, WI, 1993.
(57) Bruker *SHELXTL*, ver. 5.10; Bruker AXS: Madison, WI, 1997.
(58) Sheldrick, G. M. *SHELXS97 and SHELXL97*, University of Göttingen: Göttingen, Germany, 1997.
(59) Love, J. C.; Demas, J. N. *Anal. Chem.* **1984**, *56*, 82.

Volmer plots were extracted by a least-squares treatment of the relative intensity data.

Computational Studies. All of the calculations were done using *Gaussian 03*[60] and the B3LYP/6-31G(d) model except those calculations appearing in Table 2. All of the stationary points were checked with frequency calculations and the absence of spin contamination was verified by examination of $\langle S^2 \rangle$.

Cyclic Voltammetry. Electrochemical samples were prepared in acetonitrile and were 2×10^{-3} M in substrate, 0.1 M in supporting electrolyte (nBu_4NClO_4), and 2×10^{-3} M in ferrocene as an internal standard. Cyclic voltammograms were collected at a variety of scan rates, utilizing a three-electrode configuration including a glassy carbon working electrode, a platinum wire as a counter electrode, and a Ag/AgCl (NaCl-satd) reference electrode.

General $NMQ^+BF_4^-$ Photooxygenation Conditions. The photooxygenations of **1** (1.25×10^{-2} M) and **2** sensitized by 5 mol % $NMQ^+BF_4^-$ were carried out in dry-oxygen-agitated/saturated deuterated acetonitrile solutions in an NMR tube. A 450 W medium-pressure mercury lamp was used as the light source, and a Pyrex test tube was used as a filter (310 nm cutoff). Oxidation products were detected and monitored by either proton NMR or GCMS.

General Singlet Oxygen Photooxygenation Conditions. The photooxygenations of 0.1 M **1** sensitized by methylene blue (10^{-4} M) were carried out in oxygen-saturated deuterated acetonitrile solutions in an NMR tube. The samples were irradiated through a 1 cm saturated $NaNO_2$ filter solution with a halogen−tungsten lamp set at 250 W. The reaction mixtures were analyzed by proton NMR.

General Pyrylium Cation Photooxygenation Conditions. The photooxygenations of $1-2 \times 10^{-2}$ M of **1** or **2** with 8 mol % TPP^+, **2**MeOTPP$^+$, and **2**MeOSTPP$^+$ were carried out in oxygen-agitated/saturated deuterated acetonitrile solutions in an NMR tube. Irradiations were carried out through 1 cm of a saturated $NaNO_2$ solution with a 600 or 250 W halogen−tungsten lamp. The reaction mixtures were analyzed by either proton NMR, GC, or GCMS.

Photooxygenation of *tert*-Butylphenylsulfide. The photooxygenations of 0.1 M *tert*-butylphenylsulfide with 4×10^{-4} M NMQ^+ and 4×10^{-4} M **2**MeOTPP$^+$ were conducted in acetonitrile using 3×10^{-4} M hexamethyldisiloxane as an internal standard. The NMQ^+ reaction was irradiated with a medium-pressure Hanovia lamp for 10 min and the **2**MeOTPP$^+$ sensitized reaction was irradiated for 1 h with a 600 W halogen−tungsten lamp. Both reaction mixtures were examined by proton NMR, clearly demonstrating the formation of identical products in very similar ratios. Under these reaction conditions, 53% of the *tert*-butylphenylsulfide had reacted in the NMQ^+ reaction and 59% in the **2**MeOTPP$^+$ reaction. The major product was the *tert*-butylacetamide in both cases (17% NMQ^+, 26% 2MeOTPP$^+$). Substantial amounts of *tert*-butanol (13% NMQ^+, 21% **2**MeOTPP$^+$) and acetone (9% NMQ^+, 7% **2**MeOTPP$^+$) were also found in the reaction mixtures. Phenyl sulfonic acid and diphenyldisulfide were partially obscured by overlap with the starting material and were not quantified. When these reactions were run under identical conditions, but, in the presence of 1.2×10^{-3} M benzoquinone, less than 8% of the products were observed in the NMQ^+ reaction and no products were observed in the **2**MeOTPP$^+$ reaction.

Solvent Effects (Table 1). A 1 mL CD_3CN stock solution of the sensitizer was used to prepare a 0.5 mL CD_3CN sample containing 2 mg of **1** and 3 mol % (5×10^{-3} M) of the sensitizer. The $CDCl_3$ samples were prepared by first removing the CD_3CN under a vacuum from a 100 μL aliquot of the stock solution before adding 0.5 mL of $CDCl_3$ containing 2 mg of **1**. Both solutions were put into pyrex NMR tubes, saturated with oxygen for 3 min, and then irradiated with UVA lamps in a merry-go-round.

Acknowledgment. We thank the National Science Foundation for their generous support of this research. We also thank Dr. Doug Wheeler for development of the program *Lifetime* used to extract lifetimes from the singlet-oxygen emission data.

Supporting Information Available: Stern−Volmer quenching data of sensitizers by **1** and **2**, electrochemical data for triarylpyrylium cations in argon and oxygen, TD−DFT results for **1** and **2** radical cations, B3LYP/6-31G(d) structure data for **1** and its derivatives and for *O*-methyl dimethylpersulfoxide, and a CIF file for the X-ray analysis of **5**. This material is available free of charge via the Internet at http://pubs.acs.org.

JA710301S

(60) Frisch, M. J.; Trucks, G. W.; Schlegel, H. B.; Scuseria, G. E.; Robb, M. A.; Cheeseman, J. R.; Montgomery, J. A., Jr.; Vreven, T.; Kudin, K. N.; Burant, J. C.; Millam, J. M.; Iyengar, S. S.; Tomasi, J.; Barone, V.; Mennucci, B.; Cossi, M.; Scalmani, G.; Rega, N.; Petersson, G. A.; Nakatsuji, H.; Hada, M.; Ehara, M.; Toyota, K.; Fukuda, R.; Hasegawa, J.; Ishida, M.; Nakajima, T.; Honda, Y.; Kitao, O.; Nakai, H.; Klene, M.; Li, X.; Knox, J. E.; Hratchian, H. P.; Cross, J. B.; Bakken, V.; Adamo, C.; Jaramillo, J.; Gomperts, R.; Stratmann, R. E.; Yazyev, O.; Austin, A. J.; Cammi, R.; Pomelli, C.; Ochterski, J. W.; Ayala, P. Y.; Morokuma, K.; Voth, G. A.; Salvador, P.; Dannenberg, J. J.; Zakrzewski, V. G.; Dapprich, S.; Daniels, A. D.; Strain, M. C.; Farkas, O.; Malick, D. K.; Rabuck, A. D.; Raghavachari, K.; Foresman, J. B.; Ortiz, J. V.; Cui, Q.; Baboul, A. G.; Clifford, S.; Cioslowski, J.; Stefanov, B. B.; Liu, G.; Liashenko, A.; Piskorz, P.; Komaromi, I.; Martin, R. L.; Fox, D. J.; Keith, T.; Al-Laham, M. A.; Peng, C. Y.; Nanayakkara, A.; Challacombe, M.; Gill, P. M. W.; Johnson, B.; Chen, W.; Wong, M. W.; Gonzalez, C.; Pople, J. A. *Gaussian 03*, revision C.02; Gaussian, Inc.: Wallingford, CT, 2004.